

Study on Temperature Sensitive Characteristics of UHF Radio Frequency Identification Temperature Sensing Tag

Hongbin Ge^{*}, Yuan Yao, and Junsheng Yu

Abstract—In order to design a robust passive temperature sensing tag that can operate over a wide temperature range, temperature-sensitive characteristic of UHF radio frequency identification temperature sensing chip and corresponding tags are studied. The devices under test include dipole tags with different antenna impedances. Simulation data, experiment design, system setup, measurement procedures, and test results are given. The results show that as temperature increases, the real part of chip impedance increases, and the absolute value of the imaginary part decreases, which are consistent with simulation data. In the full temperature range, the overall performance of sensing tags designed for high-temperature conditions is better than tags designed only for room temperature conditions.

1. INTRODUCTION

Passive UHF Radio frequency identification (RFID) technology is considered promising among the existing Internet of Things (IoT) solutions due to its low cost, easy maintenance, and extended operating range. Besides the conventional identification function, researchers and manufacturers have tried to add sensing functions to it, such as temperature [1], humidity [2], pressure [3], leading to an emerging research and application area.

A typical passive UHF RFID system includes tags, readers, and software, where tags are usually composed of tag antennas and chip. The tag antenna activates the chip by receiving electromagnetic waves emitted by the reader, and the minimum activation power is often called the sensitivity of the chip. Previously, the integration of sensor modules into traditional passive RFID chips was limited by power consumption, and the working distance was close. As technology evolves, the power consumption of chips and sensor modules continues to decrease, and it is no longer a constraint on integrated on-chip sensors.

Tag performance has a crucial impact on the entire system performance. In most passive RFID tag design, first, select the appropriate chip and then design the tag antenna to cooperate with it to achieve optimal tag performance.

Since the chip contains nonlinear components such as transistors and capacitors, its input impedance is power and frequency dependent. The common practice is designing the antenna impedance as the complex conjugate of the chip impedance at the sensitivity power level in order to get maximum power transfer from the tag antenna to the chip at the possible most extended reading range.

In addition to the incident power and operating frequency, the chip input impedance also relates to the environmental parameters (e.g., temperature). The environment can affect chip and tag performance, especially for sensing chips. Therefore, it is proper to incorporate the characteristics of the sensing chip into the overall tag design.

If we aim to improve the performance of temperature sensing tag under high-temperature conditions, the straightforward idea is to measure the temperature-sensing chip impedance change

Received 26 March 2019, Accepted 22 May 2019, Scheduled 31 May 2019

^{*} Corresponding author: Hongbin Ge (buptgehongbin@126.com).

The authors are with the School of Electronic Engineering, Beijing University of Posts and Telecommunications, Beijing, China.

with temperature directly, and then design the tag antenna matching the chip according to the results. However, direct chip impedance measurement under the high-temperature condition is challenging. The final result is likely to fluctuate significantly. Measurement is easier to control and adjust at room temperature than the high-temperature condition. Accuracy cannot be guaranteed.

In this paper, we measure the overall tag performance as temperature changes, and then indirectly analyze and verify the temperature-sensitive characteristics of the chip. Design guidelines are provided for the subsequent design of robust temperature sensing tags that operate in a wide temperature range.

The structure of this paper is as follows. First, the temperature-sensitive characteristics of the chip and its simulation data are described. Then, the design, setup, and procedures of the experiment are introduced, followed by the analysis and discussions of the test results. Finally, a summary and future work are presented.

2. SIMULATIONS

In this section, we will describe the temperature sensitive characteristic of a chip and its simulation data.

Due to the physical characteristics of the chip itself, its equivalent circuit model is usually represented as a parallel combination of resistor and capacitor [4], as shown in Figure 1. Where R_p is the equivalent parallel resistance, C_p is the equivalent parallel capacitance. However, the equivalent circuit model of the dipole antenna commonly used in the tag antenna is a series combination of resistor and inductor. In order to facilitate the analysis of the overall performance of the tag, the parallel equivalent circuit of the chip is generally converted into a corresponding series equivalent circuit model. The series equivalent circuit model of the tag is shown in Figure 2, where V_{oc} is the open circuit voltage of the tag, R_{ant} and X_{ant} are the real and imaginary parts of the tag antenna impedance, respectively, and R_{chip} and X_{chip} are the real and imaginary parts of the chip impedance, respectively.

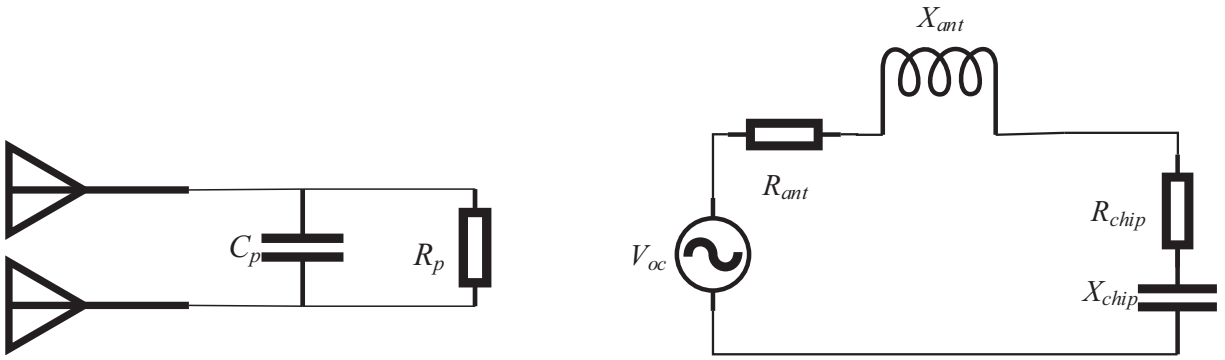


Figure 1. Chip equivalent parallel circuit model.

Figure 2. Tag equivalent series circuit model.

For a given frequency $f = \omega/2\pi$, the conversion relationship between the resistor-capacitor parallel and series equivalent circuit is

$$R_s = \frac{R_p}{1 + (\omega C_p R_p)^2}; \quad C_s = \frac{1 + (\omega C_p R_p)^2}{\omega^2 C_p R_p^2} \quad (1)$$

where R_s is the equivalent series resistance, and C_s is the equivalent series capacitance. For an equivalent series circuit, the expression of the series impedance Z_s is

$$Z_s = R_s - j \frac{1}{\omega C_s} \quad (2)$$

It can be seen from equations that in the ultra-high frequency band, the values of the equivalent series and parallel capacitors do not differ much while the series resistance value is inversely proportional to the parallel resistance: if the shunt resistance reduces, the series resistance increases, i.e., the real

part of the chip impedance increases; if the shunt capacitance increases, the series capacitance also increases, i.e., the absolute value of the imaginary part of the chip impedance reduces.

If the antenna impedance and chip impedance are known, the power transfer coefficient τ [4] between the antenna and the chip can be calculated by Equation (3), where Z_{chip} represents the chip impedance, and Z_{ant} represents the antenna impedance. The higher the power transfer coefficient, the better the match between the chip and the antenna. The maximum power transfer coefficient is 1 when the antenna impedance is conjugated to the chip impedance.

$$\tau = \frac{4R_{chip}R_{ant}}{|Z_{chip} + Z_{ant}|^2} \quad (3)$$

The temperature sensing chip used in the subsequent experiments is a passive UHF RFID temperature sensing chip (CTESIUS series LTU27 model) developed by Zhejiang JOHAR Technology Co., Ltd. The measurable temperature range of the chip is from -40°C to 125°C . The temperature measurement accuracy is 1°C , while the temperature resolution is 0.13°C .

Table 1 shows the simulation data of the equivalent parallel resistance and capacitance of the chip under different temperature conditions provided by the company, as a benchmark for subsequent discussions.

It should be noted that the data listed in Table 1 are only the preliminary data. After extracting the parasitic parameters, the value of C_p needs to increase about 0.135 pF. Considering other factors such as encapsulation and glue when making tags, it is necessary to add about 0.1 to 0.2 pF. Also, the actual R_p value may be smaller than the simulated value. The reference value of the parallel equivalent circuit model listed in the manufacturer's datasheet is $1.03\text{ k}\Omega \parallel 0.85\text{ pF}$. The simulation data show that as the temperature rises, R_p decreases and C_p rises, that is, the real part of the chip impedance increases and the absolute value of the imaginary part decreases. This trend is also consistent with the relationship between the real part of the impedance and the temperature of another UHF RFID chip measured in [5]. But in [5], the imaginary part of the chip impedance is nearly unchanged with temperature because the chip has an automatic tuning function and can adjust C_p within a certain range. The chip used in this paper doesn't have this function so we can see the variation of the C_p with the temperature in Table 1.

Empirical formulas for the relationship between R_p , C_p and temperature T can be derived based on the simulation chip impedance data presented in Table 1.

$$R_p(T) = R_{p0} + k_{1r}T + k_{2r}T^2 \quad (4)$$

$$C_p(T) = C_{p0} + k_{1c}T + k_{2c}T^2 \quad (5)$$

where $R_{p0} = 1.51\text{ k}\Omega$ is the R_p value at 0°C ; T is the temperature in $^\circ\text{C}$; and $k_{1r} = -1.46 \times 10^{-3}$ and $k_{2r} = -1.13 \times 10^{-5}$ are the coefficients of R_p as a function of temperature. The expression of C_p is similar, where $C_{p0} = 0.48\text{ pF}$ is the C_p value at 0°C ; T is the temperature in $^\circ\text{C}$; and $k_{1c} = 2.10 \times 10^{-4}$ and $k_{2c} = 1.02 \times 10^{-6}$ are the coefficients of C_p as a function of temperature.

Table 2 shows the real part R_s , imaginary part X_s , and Q of the chip series impedance corresponding to the different R_p and C_p combinations. R_p decreases, and C_p rises as the temperature rises. The step of R_p is 0.1 k Ω , and the step of C_p is 0.01 pF.

In general, the bandwidth is inversely proportional to the quality factor Q , which is the ratio of the absolute value of the imaginary part of the impedance to the real part of the impedance — the lower

Table 1. Simulation data of chip impedance as a function of temperature.

Temp/ $^\circ\text{C}$	Rp/k Ω	Cp/pF
-40	1.555	0.474
25	1.465	0.487
45	1.431	0.492
125	1.155	0.523

Table 2. Chip shunt resistor and capacitor values and equivalent series impedances @922.5 MHz.

Rp/k Ω	Cp/pF	Rs/ Ω	Xs/ Ω	Q
1.2	0.85	33.38	-197.33	5.9
1.1	0.86	35.41	-194.15	5.5
1.0	0.87	37.84	-190.80	5.0
0.9	0.88	40.77	-187.17	4.6

the Q value, the wider the relative operating bandwidth. The reason for choosing 922.5 MHz is that it is the center frequency of the China Radio Frequency Identification Standard 920–925 MHz band.

3. MEASUREMENTS

In this section, we will test the temperature-sensitive characteristics of the passive wireless temperature sensing tags based on the sensing chip. The purpose is to indirectly verify the chip impedance variation with temperature through the experiment and provide reference and design criteria for the design of robust temperature sensing tags in a wide temperature range.

The core device for measuring tag performance is Voyantic Tagformance, which generate commands compliant with the EPC Global Class1 Gen2 standard protocol to activate tags and measure the performance at each frequency point in a frequency band. In the subsequent measurement, the operating frequency range was the 860–960 MHz band, which covers the UHF RFID band approved by regulatory agencies in most countries and regions around the world.

Besides, the temperature range of the chip is $[-40, 125]^{\circ}\text{C}$, and the performance of the chip is stable in the range of $[-40, 40]^{\circ}\text{C}$ according to the datasheet. So the discrete temperature 60°C , 80°C , 100°C , 120°C are selected for the convenience of measurement without losing generality meanwhile.

This test measures the temperature-sensitive characteristics of the tags using different antenna impedances by wireless means. The antenna form is the dipole antenna commonly used for tag antenna, and the classic T-match technique is used to adjust the real and imaginary parts of the antenna impedance. According to the simulation data of Table 1 and Table 2, two antennas with antenna impedances of $30 + j220 \Omega$ and $50 + j180 \Omega$ were selected for this test.

At the frequency of 922.5 MHz, the parallel combination of resistor and capacitor conjugated to the selected antenna impedances are $1.6 \text{ k}\Omega \parallel 0.77 \text{ pF}$ and $0.7 \text{ k}\Omega \parallel 0.89 \text{ pF}$, respectively. The former suppose to perform better at room temperature than the latter. Theoretically, the $50 + j180 \Omega$ antenna will be better than the $30 + j220 \Omega$ antenna under high-temperature conditions. Subsequent measurements have verified this conjecture. Figure 3 shows the photo of the used dipole tags with 0.15 mm thick FR-4 substrate. The relative permittivity of antenna substrate material is about 4.4 at room temperature.

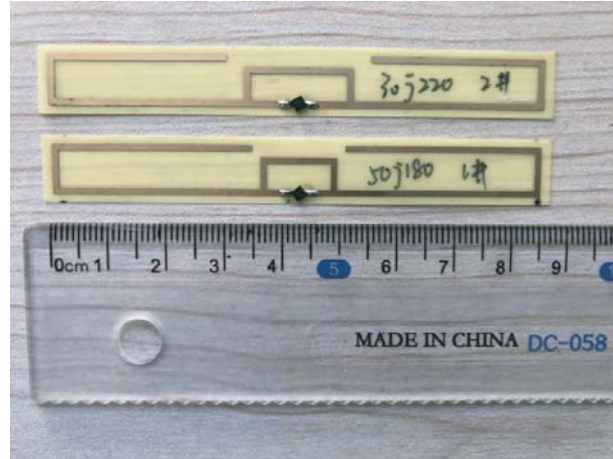


Figure 3. Photo of used dipole tags with different impedance.

It should be noted that the dielectric constant of the antenna substrate varies with temperature, and the metal material forming the antenna itself, and the antenna substrate material also has corresponding thermal expansion coefficients, which affect the antenna impedance value [5]. However, it can be considered stable with temperature in our tests due to its thickness, and even if it changes, the change is also the same proportion for both antennas. Besides, the selected two antenna impedance values have a certain degree of redundancy from each other. The change of the antenna impedance with temperature does not affect the conclusion.

The tag is placed 30 cm away from the reader antenna, fixed by a heat-resistant foam, and heated by a heat gun from the side. Use the Voyantic Tagformance to scan the forward reading distance of the tag. The frequency step is 0.5 MHz, and the power step is 0.1 dB. Before and after the measurement, another RFID reader is used to obtain the temperature value. When using the Voyantic Tagformance, the RFID reader must be turned off to prevent interference. At least two well-consistent tag samples were selected for both kinds of tags. For every sample, at least three tests were performed at each temperature point, and the results were averaged.

4. RESULTS

Figure 4 shows forward reading distance performances at 922.5 MHz with different temperature conditions. If the minimum reading distance over the entire wide temperature range is used as a measure of the overall performance of the tag, the tag with the antenna impedance of $50 + j180 \Omega$ is better than the tag with the antenna impedance of $30 + j220 \Omega$. The $50 + j180 \Omega$ tag antenna also has the benefit of a more comprehensive operating bandwidth due to its lower quality factor.

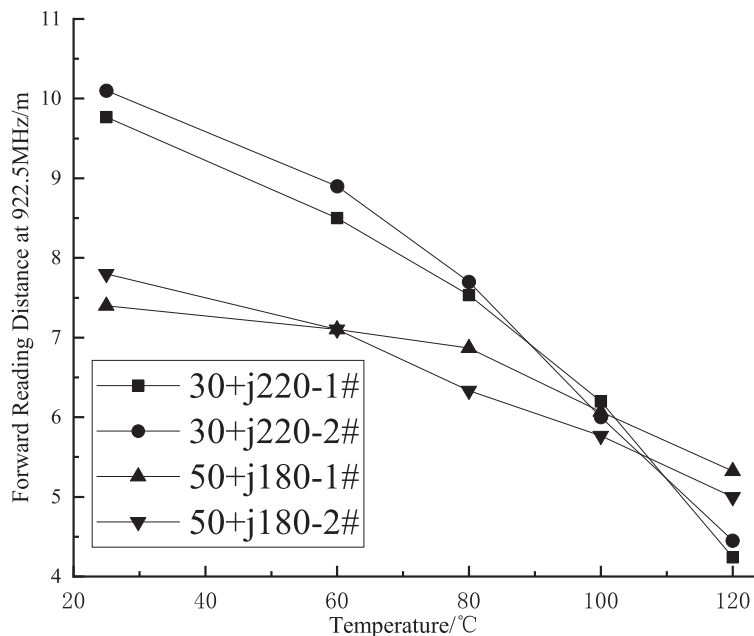


Figure 4. Forward reading distance of dipole tags with different impedances @922.5 MHz.

Figure 5 shows the forward reading distance for the tag antennas with two different impedances at 60°C and 120°C, respectively. The most representative data from the 900–930 MHz band are selected. It can be seen from Figure 5 that at 60°C, the tag with the antenna impedance of $30 + j220 \Omega$ performs better than the tag with the antenna impedance of $50 + j180 \Omega$. At 120°C, it is the opposite. The test result is consistent with our expectation.

It is worth mentioning that the relevant tests are also carried out during the cooling process of the tag from high temperature to low temperature, and the results are consistent with the test results obtained from the heating process from low temperature to high temperature.

5. DISCUSSIONS

Through the measurements, the performances of the temperature sensing tags under different temperature conditions are quantified. It is verified that as the temperature rises, the real part of the chip impedance increases, and the absolute value of the imaginary part decreases, which are consistent with the simulation data.

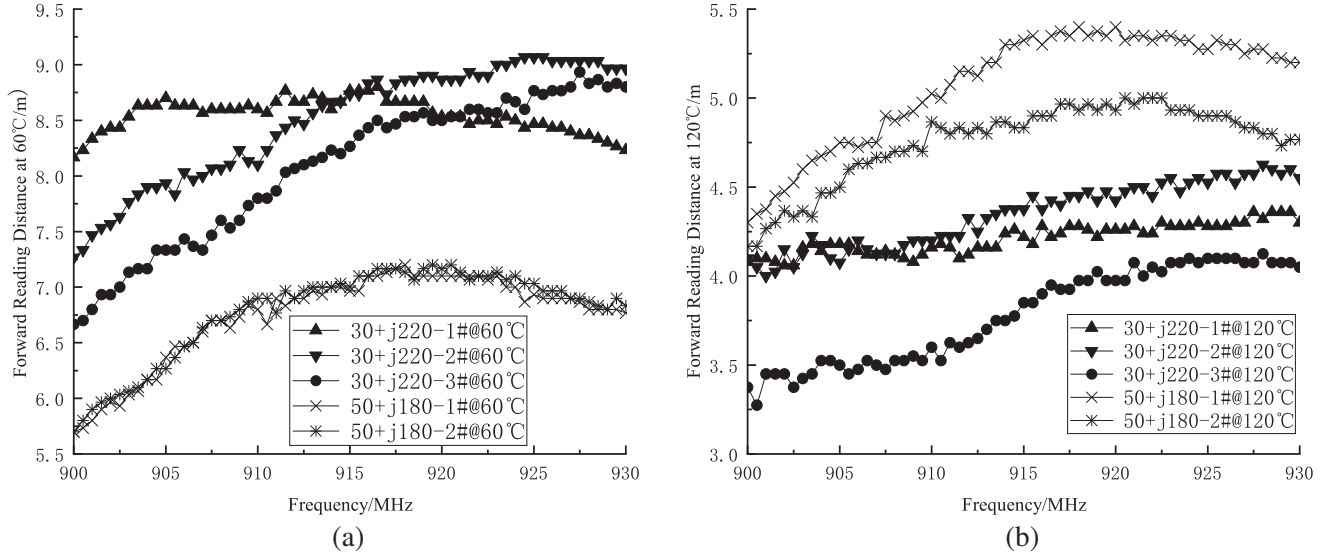


Figure 5. Forward reading distance of dipole tags with different impedances at (a) 60°C and (b) 120°C.

The temperature-sensing tag designed for chip impedance under high-temperature conditions performs better than the temperature sensing tag designed only for room temperature conditions in a wide temperature range. If the temperature sensing tag is expected to work in a harsh high-temperature environment, consider designing the tag antenna as corresponding impedance, not the best impedance at room temperature.

If the evaluation criteria are the overall performance (e.g., the minimum operating distance) over the entire temperature range, it is recommended that the tag antenna is designed to be more adaptive to high-temperature conditions, even though performance at low temperature is sacrificed to some extent. However, in exchange, the overall performance of the temperature sensing tag is more stable and reliable over the entire operating temperature range.

6. CONCLUSIONS

The measured results in this paper provide reference and design ideas for the robust temperature sensing tags in the full temperature range. In future work, the method of measuring chip impedance in [6] can be improved to measure the relationship between chip impedance and temperature directly and cross-validate the results of this paper.

Alternatively, we can also explore how to accurately measure the optimal antenna impedance corresponding to the temperature change, and design the tag antenna accordingly.

Furthermore, it is possible to use a suitable temperature sensitive material as the antenna dielectric substrate, so that the antenna can adaptively adjust the antenna impedance within a certain range according to temperature changes to improve the overall performance of the temperature sensing tag.

ACKNOWLEDGMENT

The authors would like to thank Dr. Jun Yi, CTO of Zhejiang JOHAR Technology Co., Ltd., and his colleagues for their help in this project.

REFERENCES

1. Babar, A. A., S. Manzari, L. Sydanheimo, A. Z. Elsherbeni, and L. Ukkonen, "Passive UHF RFID tag for heat sensing applications," *IEEE Transactions on Antennas and Propagation*, Vol. 60, No. 9, 4056–4064, 2012.

2. Strangfeld, C., S. Johann, M. Müller, and M. Bartholmai, “Embedded passive RFID-based sensors for moisture monitoring in concrete,” *IEEE Sensors*, 1–3, 2017.
3. Fernandez, I., A. Asensio, I. Gutierrez, J. Garcia, I. Rebollo, and J. de No, “Study of the communication distance of a MEMS pressure sensor integrated in a RFID passive tag,” *Advances in Electrical and Computer Engineering*, Vol. 12, No. 1, 15–18, 2012.
4. Dobkin, D. M., *The RF in RFID: UHF RFID in Practice*, Newnes, 2012.
5. Zannas, K., H. El Matbouly, Y. Duroc, and S. Tedjini, “Self-tuning RFID tag: A new approach for temperature sensing,” *IEEE Transactions on Microwave Theory and Techniques*, Vol. 66, No. 12, 5885–5893, 2018.
6. Heiss, M., “Wireless RFID chip impedance measurement by using an reader and a statistically analysis,” *Smart SysTech*, 1–7, 2012.